Introduction

A. Bunyatyan[1,2]*, A. Cooper-Sarkar*[3]*, C. Diaconu*[4,5]*, R. Engel*[6]*, C. Kiesling*[7]*, K. Kutak*[4]*,*
S. Ostapchenko[8,9]*, T. Pierog*[4]*, T.C. Rogers*[10]*, M.I. Strikman*[10]*, T. Sako*[11]*.*

[1] MPI, Heidelberg, Germany
[2] Yerevan Physics Institute, Armenia
[3] Oxford University, Dept of Physics, Oxford, UK
[4] DESY, Hamburg, Germany
[5] CPPM, Marseille, France
[6] Forschungszentrum Karlsruhe, Institut für Kernphysik, Karlsruhe, Germany
[7] Max-Planck-Institute for Physics, München, Germany
[8] Institutt for fysikk, NTNU Trondheim, Norway
[9] D. V. Skobeltsyn Institute of Nuclear Physics, Moscow State University, Russia
[10] Pennsylvania State University, United States
[11] Solar-Terrestrial Environment Laboratory, Nagoya University, Nagoya, Japan

Abstract

When particle physic started, cosmic ray were used as source of new particles. Nowadays particle physic is a fundamental key to understand the nature of the very high energy cosmic rays. Above 10^{14} eV, primary cosmic rays are detected via air showers whose development strongly rely on the physic of the forward region of hadronic interactions as tested in the HERA and LHC experiments. After an introduction on air shower phenomenology, we will review how HERA and LHC can constrain the physic used both in hadronic interaction model, or for photon or neutrino primaries.

1 Physics questions and problems

One of the central questions of astroparticle physics is that of the sources and propagation of cosmic rays. Even more than 90 years after the discovery of cosmic rays we still don't know their elemental composition at high energy and also the information on the energy spectrum is very limited [1–6]. Knowing the cosmic-ray composition is the key to understanding phenomena such as the *knee*, a change in the power-law index of the cosmic ray flux at about 3×10^{15} eV, the transition from galactic to extra-galactic cosmic rays, and the implications of the existence of ultra-high energy cosmic rays with $E > 10^{20}$ eV. In particular, composition information is essential for confirming or ruling out models proposed for the sources of ultra-high energy cosmic rays, many of which postulate new particle physics [7, 8].

The flux of cosmic rays is shown in Fig. 1 in the energy range from 10^{12} eV up to the highest energies. It has been scaled by $E^{2.5}$ to make the characteristic features of the spectrum clearly visible. In addition the equivalent energies of colliders, referring to proton-proton collisions, are indicated by arrows.
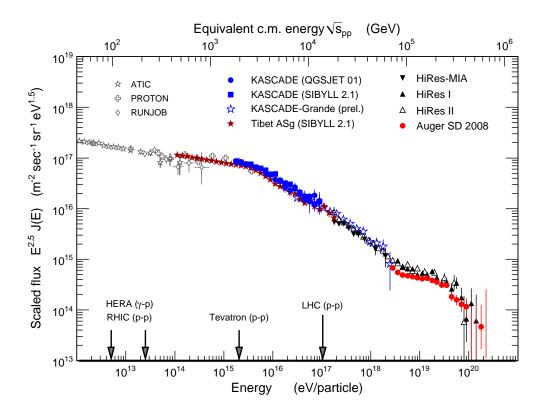
Fig. 1: All-particle flux of cosmic rays as obtained by direct measurements above the atmosphere by the ATIC [9], PROTON [10, 11], and RUNJOB [12] as well as results from air shower experiments. Shown are Tibet ASγ results obtained with SIBYLL 2.1 [13], KASCADE data (interpreted with two hadronic interaction models) [14], preliminary KASCADE-Grande results [15], and Akeno data [16, 17]. The measurements at high energy are represented by HiRes-MIA [18, 19], HiRes I and II [20], and Auger [21].

The all-particle spectrum can be approximated by a broken power law $\propto E^\gamma$ with a spectral index $\gamma = -2.7$ below $E_k \approx 4 \times 10^{15}$ eV. At the *knee*, the spectral index changes to $\gamma \approx -3.1$. The power law index changes again at about $10^{18.5}$ eV, a feature that is called the *ankle*. At the very high end of the spectrum there seems to be a suppression of the flux. None of these features of the energy spectrum of cosmic rays is understood so far. In the following some of the related theoretical questions and models are presented for illustration.

- **Knee.** At the knee, the cosmic ray spectrum changes in a way that is very difficult to understand in models with a superposition of different sources, each producing a power-law flux. The knee could be feature of the acceleration process, it could be the result of propagation effects from the sources to Earth (leakage from the Galaxy), or it could be caused by new particle physics. Knowing the change of the elemental composition of cosmic rays through the knee energy region will help to distinguish some of the possible scenarios. Acceleration and propagation models of the knee predict that the spectra of individual elements should each exhibit a knee, however at an energy that is scaled by the

charge of the particle due to the coupling to astrophysical magnetic fields (for example, [22]). In contrast, models postulating new interaction physics (for example, [23]) and the *cannon ball* model [24] predict a scaling proportional to the number of nucleons of the nucleus (i.e. mass number). A review of the different scenarios and their predictions can be found in, for example, [25].

- **Ankle.** The ankle is often regarded as a signature of the transition from Galactic to extragalactic cosmic rays. Such a transition is expected in this energy range because of the strength of the Galactic magnetic fields being of the order of 3 μG [26]. Particles with energies above 10^{19} eV are not confined to the Galaxy. The exact energy of the transition is not known [27]. In the dip model the ankle is a result of the propagation of ultra-high energy cosmic rays through the microwave background radiation [28,29]. Within this model, ultra-high energy cosmic rays have to be dominated by protons. Other models of the ankle explain the feature in the spectrum by the superposition of different power laws from Galactic and extragalactic sources [4,30,31]. In such a scenario the composition would most likely be mixed with contributions from both light and heavy elements, i.e. in the range from protons to iron nuclei.

- **Upper end of the spectrum.** A strong suppression of the particle flux above $E = 7 \times 10^{19}$ eV is expected from the interaction of cosmic rays with the cosmic microwave background radiation, the Greisen-Zatsepin-Kuzmin (GZK) effect [32, 33]. Both protons and nuclei suffer significant energy losses when propagating over distances larger than ~ 100 Mpc. On the other hand, the sources could have reached their upper limit of acceleration or injection power and we would be mistaken by attributing the observations just to the GZK suppression. In any case the sources of such high energy particles have to be rather exotic [34]. One would have to build the LHC with a circumference of the length of the orbit of the planet Mercury to reach the same energy with the currently available technology. Particles of such energies also probe Lorentz invariance at extreme energies [35, 36] and hence allow to search for space-time fluctuations (for example, see [37, 38]).

To solve these questions, multi-messenger and multi-observable measurements are needed. First of all, the flux, composition and arrival direction distribution of cosmic rays will have to measured with high statistics and precision. Secondly, complementary information obtained from observing secondary particle fluxes (gamma-rays and neutrinos) will greatly help to disentangle different source and propagation scenarios [39, 40].

At energies above 10^5 GeV, the flux of cosmic rays is so low that it cannot be measured directly using particle detectors. Therefore all cosmic-ray measurements of higher energy are based on analyzing the secondary particle showers, called extensive air showers, which they produce in the atmosphere of the Earth. To interpret the characteristics of extensive air showers in terms of primary particle type and energy, detailed modeling of the various interaction and decay processes of the shower particles is needed (for example, see [41, 42]). In particular, the elemental composition of the cosmic-ray flux reconstructed form air shower data depends very much on the assumptions on hadronic multiparticle production.

2   Air shower phenomenology and hadronic interactions

A commonly employed technique to observe air showers is the measurement of secondary particles (electrons, photons and muons) reaching the ground [2]. Using an array of particle detectors (for example, sensitive to $e^\pm$ and $\mu^\pm$), the arrival direction and information on mass and energy of the primary cosmic ray can be reconstructed. The main observables are the number and the lateral and temporal distributions of the different secondary particles. At energies above $\sim 10^{17}$ eV, the longitudinal profile of a shower can be directly observed by measuring the fluorescence light induced by the charged particles traversing the atmosphere [43]. Two main observables can be extracted from the longitudinal shower profile: the energy deposit or the number of particles, $N_{\max}$, at the shower maximum and $X_{\max}$, the atmospheric depth of the maximum. Again, these quantities can be used to estimate the energy and mass of the primary particles. Shower-to-shower fluctuations of all observables make it impossible to derive the mass of the primary particle on a shower-to-shower basis. On the other hand, these fluctuations provide very useful and complementary composition information.

To qualitatively understand the dependence of the air shower development on some basic parameters of particle interaction, decay, and production, a very simple toy model can be used. Although initially developed for electromagnetic (EM) showers [44] it can also be applied to hadronic showers [45].

First we consider a simplified electromagnetic shower of only one particle type. A particle of energy E produces in an interaction two new particles of the same type with energies $E/2$, after a fixed interaction length of λ_e. With n being the number of generations (consecutive interactions), the number of particles at a given depth $X = n \cdot \lambda_e$ follows from

$$N(X) = 2^n = 2^{X/\lambda_e}, \tag{1}$$

with the energy E per particle for a given primary energy E_0 being

$$E(X) = \frac{E_0}{2^{X/\lambda_e}}. \tag{2}$$

Defining the critical energy E_c (~ 85 MeV in air) as the energy below which continuous energy loss processes (i.e. ionization) dominate over particle production, one can make the assumption that the shower maximum is reached at a depth at which the energy of the secondary particles is degraded to E_c. Then two main shower observables are given by

$$N_{\max} = \frac{E_0}{E_c} \quad \text{and} \quad X_{\max}^e(E_0) \sim \lambda_e \cdot \ln\left(\frac{E_0}{E_c}\right). \tag{3}$$

Of course, this very simplified picture does not reproduce the detailed behavior of an EM shower, but two important features are well described: the number of particles at shower maximum is proportional to E_0 and the depth of shower maximum depends logarithmically on the primary energy E_0.

Generalizing this idea, a hadronic interaction of a particle with energy E is assumed to produce n_{tot} new particles with energy E/n_{tot}, two third of which being charged particles n_{ch} (charged pions) and one third being neutral particles n_{neut} (neutral pions). Neutral particles decay

immediately into em. particles particles ($\pi^0 \to 2\gamma$), feeding the em. shower component. After having traveled a distance corresponding to the mean interaction length λ_{ine}, charged particles re-interact with air nuclei as long as their energy exceeds some typical decay energy E_{dec}.

In the end, most of the energy of an air shower is carried by em. particles ($\sim 90\%$ for $n = 6$). The depth of shower maximum is given by that of the em. shower component, X_{max}^e. As the first hadronic interaction produces em. particles of energy $\sim E_0/n_{\text{tot}}$ one gets

$$X_{\text{max}}(E_0) \quad \sim \quad \lambda_{\text{ine}} + X_{\text{max}}^e(E_0/n_{\text{tot}}) \tag{4}$$

$$\sim \quad \lambda_{\text{ine}} + \lambda_e \cdot \ln\left(\frac{E_0}{n_{\text{tot}} E_c}\right), \tag{5}$$

where λ_{ine} is the hadronic interaction length. This simplified expression for the shower depth of maximum neglects the em. sub-showers initiated by hadrons of later generations. The inclusion of higher hadronic generations does not change the structure of Eq. (5), see [46].

Following [45], we assume that all charged hadrons decay into muons when their energy reaches E_{dec}. By construction, charged particles will reach the energy E_{dec} after n interactions

$$E_{\text{dec}} = \frac{E_0}{(n_{\text{tot}})^n}. \tag{6}$$

Since one muon is produced in the decay of each charged particle, we get for the number of muons in an hadronic shower

$$N_\mu = n_{\text{ch}}^n = \left(\frac{E_0}{E_{\text{dec}}}\right)^\alpha, \tag{7}$$

with $\alpha = \ln n_{\text{ch}}/\ln n_{\text{tot}} \approx 0.82\ldots0.95$ [46, 47]. The number of muons produced in an air shower depends not only on the primary energy and air density, but also on the charged and total particle multiplicities of hadronic interactions.

In case of showers initiated by nuclei, one can use the superposition model to deduce the expectation value for inclusive observables [48]. In this model, a nucleus with mass A and energy E_0 is considered as A independent nucleons with energy $E_{\text{h}} = E_0/A$. This leads to

$$N_{\text{max}}^A \quad \approx \quad A \cdot \frac{E_{\text{h}}}{E_c} = \frac{E_0}{E_c} = N_{\text{max}} \tag{8}$$

$$X_{\text{max}}^A \quad \approx \quad X_{\text{max}}(E_0/A) \tag{9}$$

$$N_\mu^A \quad \approx \quad A \cdot \left(\frac{E_0/A}{E_{\text{dec}}}\right)^\alpha = A^{1-\alpha} \cdot N_\mu. \tag{10}$$

There is no mass dependence of the number of charged particles at shower maximum. The number of muons and the depth of maximum depend on the mass of the primary particle. The heavier the shower-initiating particle the more muons are expected for a given primary energy. For example, an iron-induced shower has about 1.4 times more muons than a proton shower of the same energy.

There are several code packages available for performing Monte Carlo simulations of extensive air showers. The more frequently used programs are AIRES [50], CORSIKA [51],
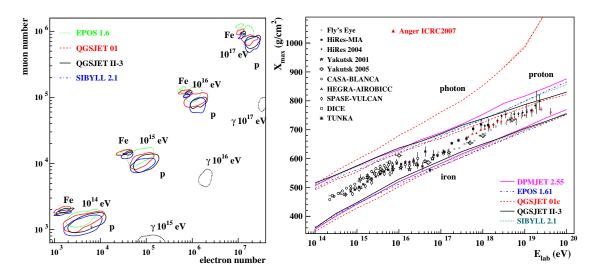
Fig. 2: Predictions for air shower observables for proton-, iron- and photon-induced showers. Left panel: Shown are the correlation between the number of electrons and muons at ground as expected with different hadronic interaction models (see text) [49]. Right panel: compilation of data of the mean depth of shower maximum and model predictions [49].

CONEX [52], SENECA [53], MOCCA [54], and COSMOS [55]. These packages provide either self-made hadronic interaction models that cover the full energy range from the particle production threshold to the highest energies or employ external models for the simulation of these interactions. Due to the different methods of modeling, external hadronic interaction models are typically optimized for low- or high-energy interactions.

Low-energy models describe hadronic interactions in terms of intermediate resonances (for example, the isobar model) and parametrizations of data. They are applicable in the energy range from the single particle production threshold up to several hundred GeV. Models that are often applied in simulations are FLUKA (which is a complete cascade simulation package that includes both low- and high-energy models) [56], GHEISHA [57], UrQMD [58], and the more specialized code SOPHIA [59]. Low-energy models are typically well-tuned to the large number of data sets from fixed target measurements. Still the differences between the model predictions are significant and can lead to very different muon densities in air shower simulations [60, 61].

High-energy interaction models are typically very complex models and based on Regge theory [62], Gribov's Reggeon calculus [63], and perturbative QCD. Central elements of these models are the production of QCD minijets and the formation of QCD color strings that fragment into hadrons. The most frequently used models are QGSJET 01 [64, 65] and II [66, 67], SIBYLL 2.1 [48, 68, 69], EPOS 1.6 [70, 71] and DPMJET II [72] and III [73, 74]. The extrapolation of these models to very high energy depends on the internal structure of the model and the values of the tuned model parameters and is, in general, rather uncertain. Different extrapolations obtained within one model by varying the parameters can be found in [75, 76] and represent only a lower limit to the uncertainty of the predictions.

Monte Carlo models typically applied in high energy physics are not used for air shower

simulations. Most of these models do not allow the simulation of particle production with air nuclei as target or are applicable in a rather limited energy range (however, see [77] for a study with HIJING [78]).

Detailed numerical simulations of extensive air showers confirm the overall functional relations between the shower energy, depth of shower maximum, and number of electrons and muons that have been derived within the simple Heitler-Matthews model. The expected correlation between the number of electrons and muons at a surface detector at sea level is shown in Fig. 2. The simulations were made for vertical showers with the air shower simulation package CORSIKA [51]. The predictions obtained for the interaction models QGSJET 01, QGSJET II.03, SIBYLL 2.1, and EPOS 1.6 are compared. While there is a reasonable discrimination power at low energy, the model-induced uncertainties do not allow us to discriminate between even the most extreme composition assumptions at ultra-high energy if only the number of muons and electrons is measured. The situation seems to be a somewhat better in case of the mean depth of shower maximum, but the model uncertainties are still very large.

It can be concluded from both simple cascade models of air showers and numerical studies [54,75,76,79] that the following characteristics of hadronic interactions are of central importance to air shower predictions

- Inelastic cross section for proton-air and pion/kaon-air interactions,
- Ratio between neutral and charged secondary particles (in other words, π^0 and all other particles),
- Energy distribution of the most energetic secondary particles,
- Multiplicity of high energy secondary particles,
- Scaling or scaling violation of secondary particle distributions,
- Cross section for diffractive dissociation (i.e. low-multiplicity events).

It is clear that hadronic interactions at both high and low energies are influencing the model predictions for air showers. Low-energy interactions do not influence the depth of shower maximum very much but are of direct relevance to the muon density at large lateral distance from the shower core, see [60, 61, 80].

3 Limitations of air shower simulations

Before discussing shortcomings of air shower simulations it has to be emphasized that modern simulation packages provide a very good overall description of air shower observables. The situation has very much improved in comparison to the early days of air shower simulation [81].

Modern cosmic-ray detectors like KASCADE [82] and the Pierre Auger Observatory [83] measure several observables for each shower. By choosing different observables, the model dependence of the reconstructed energy and primary particle mass can be estimated. Studies show that the uncertainty in interpreting the data from these experiments is dominated by the uncertainty in predicting hadronic multi-particle production in extensive air showers. In the following we will discuss some representative examples that illustrate the limitations of currently available hadronic interaction models and air shower simulation tools.

The KASCADE Collaboration analyzed the measured number of electrons and muons at detector level to derive the primary energy and composition of the showers in the knee energy
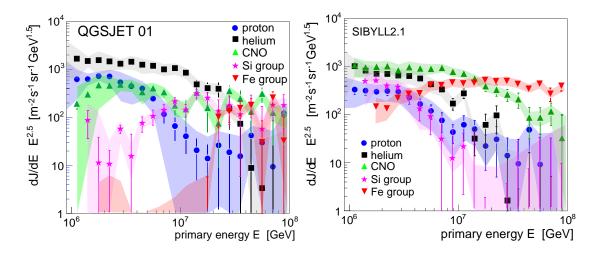
Fig. 3: Cosmic-ray flux for five elemental groups in the knee energy range as derived from KASCADE data using the hadronic interaction models QGSJET 01 (left panel) and SIBYLL 2.1 (right panel) [82].

region. Having collected more than 40 million showers it is still not possible to obtain a clear picture of the elemental composition [14]. Applying different hadronic interaction models leads to significantly different fluxes for the elemental groups considered in the analysis, see Fig. 3. In particular, the fundamental question of having a mass- or charge-dependent scaling of the knee positions of the individual flux components cannot be answered. Moreover, in an earlier study the KASCADE Collab. showed that selecting different observables gives inconsistent composition results even if the same hadronic interaction model is employed in the analysis [84].

A comparison of the world data set on electron-muon based and $X_{\max}$ based composition measurements, using the same hadronic interaction models, shows a systematic inconsistency between composition results based on surface detector data and that based on the measurement of the mean depth of shower maximum [85]. Analysis of the surface detector data indicate a heavier primary composition than one would expect from $\langle X_{\max} \rangle$ data. This is most clearly found in experiments that measure both $X_{\max}$ and an observable related to the number of muons. For example, the prototype experiment HiRes-MIA [86] studied showers in the energy range from 10^{17} to $10^{18.5}$ eV. The measured muon densities at $600\,\mathrm{m}$ from the core could only be interpreted as iron-dominated composition, but the mean $X_{\max}$ indicated a transition to a proton-dominated composition [19].

The analysis of Auger data with QGSJET II [87] leads to a similar discrepancy at an energy of about 10^{19} eV. Using universality features of very high energy showers $E > 10^{18}$ eV, one can relate the electromagnetic shower size at a lateral distance of $1000\,\mathrm{m}$ to the shower energy and the depth of shower maximum [88, 89]. The employed universality features are the same for showers simulated with the interaction models QGSJET II and SIBYLl 2.1. Considering showers at different angles and employing the independently measured depth of shower maximum, the observed muon signal can be set in relation to the predicted muon signal as shown in Fig. 4. Adopting the nominal energy scale of the Auger fluorescence detectors, the number of muons at $1000\,\mathrm{m}$ from the core is found to be twice as large as predicted by simulations with proton
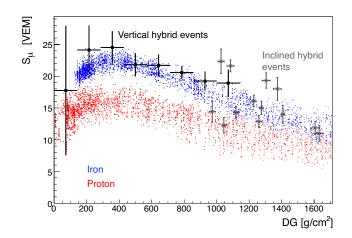
Fig. 4: Simulated and derived muon density as function of the detector depth relative to the depth of shower maximum, DG. The muon density is derived from Auger data at a distance of 1000 m from the shower core. The points show the prediction of simulations with QGSJET II and an energy increased by 30% relative to the reconstructed numinal shower energy, for details see [87].

showers. This number should be compared to that of iron-induced showers for which one expects a muon number increased by the factor 1.38 (QGSJET II) or 1.27 (SIBYLL 2.1). Increasing the energy scale by 30% as the constant intensity cut analysis of the data suggests and assuming a iron dominated composition seems to bring the surface detector data almost into agreement with the model predictions. On the other hand, the measured $\langle X_{\max} \rangle$ data is at variance with an iron-dominated composition hypothesis at 10^{19} eV.

4 Main sources of model uncertainties

In the foreseeable future soft multi-particle production will not be calculable within QCD. Therefore the modeling of cosmic-ray interactions will continue to strongly depend on the input from accelerator experiments. There are two principal types of input needed for model building. First of all, data on cross sections, secondary particle distributions and multiplicities, as well as parton densities form the basis for tuning the parameters of the models. Secondly, guidance from further development and experimental verification of theoretical and phenomenological concepts and ideas will be crucial for model development.

At the current stage even the most fundamental question of scaling of secondary particle distributions in the forward phase space region cannot be answered[1]. Within some models very strong scaling violation of the distribution of leading particles is expected [90]. So far there is no experimental proof of such a scenario. If realized in nature, the implications will be profound and most of the very high energy cosmic ray data will have to be interpreted in terms of a light composition. The lack of data on hadron production in forward direction, with the exception of HERA measurements, is one of the main source of model uncertainties. The HERA measure-

---

[1]Feynman scaling is, of course, violated for central particle production.

ments of leading proton and neutron distributions are the only high energy data available and indicate surprisingly small scaling violations [91]. It has to be expected that the leading particle distribution is correlated with the centrality of the interaction, as found in heavy ion collisions. LHC data from the big experiments [92] and LHCf [93] will be of decisive importance in this respect.

The energy fraction transferred in an interaction to particles of very short lifetime, that decay to photons and electrons, is of direct relevance to air shower simulations. Currently the particle distribution of neutral pions is derived indirectly from the distributions of charged secondaries. With the exception of the UA7 [94], no high energy data of secondary π^0 and photon distributions exist.

The extrapolation of the total and inelastic cross sections is currently hampered by the discrepant measurements from Tevatron experiments. Extrapolating the model cross section based on the CDF data [95] gives different air shower predictions than using the E710 [96] and E811 [97] data [76]. The measurement of the proton-proton cross section at LHC will reduce this uncertainty very much. Related to this cross section is, of course, the question of pion-proton and kaon-proton cross sections. The highest energy data available for the pion-nucleus cross section is that of SELEX [98]. There is no generally accepted theoretical model of how to extrapolate the ratio between proton-proton and meson-proton cross sections.

One further source of uncertainty stems from the fact that hadronic cross sections and secondary particle distributions are needed for the interaction with light nuclei in air shower simulations. At high energy, the calculation of such nuclear cross sections and particle distributions is not straightforward. At low energy, the Glauber approximation [99] is known to work remarkably well. Already the low-energy data indicates, however, the need for inelastic screening corrections for the calculation of which no reliable framework exists. For example, cross sections estimates based on air shower data indicate smaller particle production cross sections than current model extrapolations (see compilation in [100]).

One of the central theoretical questions that has to be addressed in all hadronic interaction models is that of the range of applicability of perturbative QCD. At high energy, most hadrons are produced in the fragmentation of minijets. It is of great importance to understand the correlations between individual parton-parton interactions, to which degree they can be considered independent from each other, their kinematic and color flow link to the remnants of the incoming hadrons, and the minimum momentum transfer for which such a picture can be applied. Closely related to this question is the modeling of non-linear effects in the low-x parton evolution and possible saturation or high-density shadowing effects. HERA data is of direct relevance in this respect as are RHIC measurements too. A high density of partons can also influence string fragmentation and modify particle yields relative to those measured at low energy. There are different model predictions that address this point (see, for example, [70, 101–103]) but the experimental data are not conclusive.

References

[1] S. P. Swordy *et al.*, Astropart. Phys. **18**, 129 (2002), `astro-ph/0202159`.

[2] A. Haungs, H. Rebel, and M. Roth, Rept. Prog. Phys. **66**, 1145 (2003).

[3] R. Engel and H. Klages, Comptes Rendus Physique **5**, 505 (2004).

[4] A. M. Hillas, J. Phys. **G31**, R95 (2005).

[5] K.-H. Kampert, Nucl. Phys. Proc. Suppl. **165**, 294 (2007),
    `arXiv:astro-ph/0611884`.

[6] K.-H. Kampert, J. Phys. Conf. Ser. **120**, 062002 (2008), `arXiv:0801.1986`
    `[astro-ph]`.

[7] P. Bhattacharjee and G. Sigl, Phys. Rev. **D51**, 4079 (1995), `astro-ph/9412053`.

[8] D. F. Torres and L. A. Anchordoqui, Rept. Prog. Phys. **67**, 1663 (2004),
    `astro-ph/0402371`.

[9] ATIC-2 Collaboration, H. S. Ahn *et al.* Prepared for 28th International Cosmic Ray
    Conference (ICRC 2003), Tsukuba, Japan, 31 Jul - 7 Aug 2003, 1853-1856.

[10] N. L. Grigorov *et al.*, Yad. Fiz. **11**, 1058 (1970).

[11] N. L. Grigorov *et al.* Proc. of 12th Int. Cosmic Ray Conf. (Hobart), vol. 2, p. 206, 1971.

[12] RUNJOB Collaboration, V. A. Derbina *et al.*, Astrophys. J. **628**, L41 (2005).

[13] Tibet ASγ Collaboration, M. Amenomori *et al.*, Astrophys. J. **678**, 1165 (2008),
    `arXiv:0801.1803 [hep-ex]`.

[14] KASCADE Collaboration, T. Antoni *et al.*, Astropart. Phys. **24**, 1 (2005),
    `astro-ph/0505413`.

[15] A. Haungs *et al.* To appear in Proc. of XIV ISVHECRI 2006, Weihai, China, 2006.

[16] M. Nagano *et al.*, J. Phys. **G10**, 1295 (1984).

[17] M. Nagano *et al.*, J. Phys. **G18**, 423 (1992).

[18] HiRes-MIA Collaboration, T. Abu-Zayyad *et al.*, Astrophys. J. **557**, 686 (2001),
    `astro-ph/0010652`.

[19] HiRes-MIA Collaboration, T. Abu-Zayyad *et al.*, Phys. Rev. Lett. **84**, 4276 (2000),
    `astro-ph/9911144`.

[20] HiRes Collaboration, R. Abbasi *et al.*, Phys. Rev. Lett. **100**, 101101 (2008),
    `arXiv:astro-ph/0703099`.

[21] Pierre Auger Collaboration, J. Abraham *et al.*, Phys. Rev. Lett. **101**, 061101 (2008),
    `arXiv:0806.4302 [astro-ph]`.

[22] E. G. Berezhko and H. J. Voelk (2007), `arXiv:0704.1715 [astro-ph]`.

[23] A. A. Petrukhin, Nucl. Phys. Proc. Suppl. **151**, 57 (2006).

[24] A. Dar and A. De Rujula, Phys. Rep. **466**, 179 (2006), `arXiv:hep-ph/0606199`.

[25] J. R. Hoerandel, Astropart. Phys. **19**, 193 (2003), `arXiv:astro-ph/0210453`.

[26] J. L. Han, Nucl. Phys. Proc. Suppl. **175-176**, 62 (2008).

[27] C. De Donato and G. A. Medina-Tanco (2008), `arXiv:0807.4510 [astro-ph]`.

[28] V. S. Berezinsky, S. I. Grigorieva, and B. I. Hnatyk, Astropart. Phys. **21**, 617 (2004), `astro-ph/0403477`.

[29] R. Aloisio *et al.*, Astropart. Phys. **27**, 76 (2007), `astro-ph/0608219`.

[30] T. Wibig and A. W. Wolfendale, J. Phys. **G31**, 255 (2005), `astro-ph/0410624`.

[31] D. Allard, E. Parizot, and A. V. Olinto, Astropart. Phys. **27**, 61 (2007), `astro-ph/0512345`.

[32] K. Greisen, Phys. Rev. Lett. **16**, 748 (1966).

[33] G. T. Zatsepin and V. A. Kuzmin, J. Exp. Theor. Phys. Lett. **4**, 78 (1966).

[34] A. M. Hillas, Ann. Rev. Astron. Astrophys. **22**, 425 (1984).

[35] S. R. Coleman and S. L. Glashow, Phys. Rev. **D59**, 116008 (1999), `hep-ph/9812418`.

[36] W. Bietenholz (2008), `arXiv:0806.3713 [hep-ph]`.

[37] F. R. Klinkhamer (2007), `arXiv:0710.3075 [hep-ph]`. Invited talk at 3rd Mexican Meeeting on Mathematicsal and Experimental Physics, Mexico City, Mexico, 10-14 Sep 2007.

[38] S. T. Scully and F. W. Stecker (2008), `arXiv:0811.2230 [astro-ph]`.

[39] W. Hofmann, J. Phys. Conf. Ser. **120**, 062005 (2008).

[40] J. K. Becker, Phys. Rept. **458**, 173 (2008), `arXiv:0710.1557 [astro-ph]`.

[41] J. Knapp, D. Heck, S. J. Sciutto, M. T. Dova, and M. Risse, Astropart. Phys. **19**, 77 (2003), `arXiv:astro-ph/0206414`.

[42] L. Anchordoqui *et al.*, Ann. Phys. **314**, 145 (2004), `hep-ph/0407020`.

[43] Fly's Eye Collaboration, R. M. Baltrusaitis *et al.*, Nucl. Instrum. Meth. **A240**, 410 (1985).

[44] W. Heitler, *The Quantum Theory of Radiation*, third edition[th] edn. Oxford University Press, London, 1954.

[45] J. Matthews, Astropart. Phys. **22**, 387 (2005).

[46] J. Alvarez-Muniz, R. Engel, T. K. Gaisser, J. A. Ortiz, and T. Stanev, Phys. Rev. **D66**, 033011 (2002), `astro-ph/0205302`.

[47] T. Pierog, R. Engel, and D. Heck, Czech. J. Phys. **56**, A161 (2006), `arXiv:astro-ph/0602190`.

[48] J. Engel, T. K. Gaisser, T. Stanev, and P. Lipari, Phys. Rev. **D46**, 5013 (1992).

[49] D. Heck. Talk given at CORSIKA School 2008, see http://www-ik.fzk.de/corsika/corsika-school2008/ and private communication, 2008.

[50] S. J. Sciutto (1999), `astro-ph/9911331`.

[51] D. Heck, J. Knapp, J. Capdevielle, G. Schatz, and T. Thouw, *CORSIKA: a Monte Carlo code to simulate extensive air showers* (unpublished). Wissenschaftliche Berichte FZKA 6019, Forschungszentrum Karlsruhe, 1998.

[52] T. Bergmann *et al.*, Astropart. Phys. **26**, 420 (2007), `astro-ph/0606564`.

[53] H.-J. Drescher and G. R. Farrar, Phys. Rev. **D67**, 116001 (2003), `astro-ph/0212018`.

[54] A. M. Hillas, Nucl. Phys. Proc. Suppl. **52B**, 29 (1997).

[55] K. Kasahara *et al.*, *COSMOS* (unpublished). Http://cosmos.n.kanagawa-u.ac.jp/cosmosHome.

[56] F. Ballarini *et al.*, J. Phys. Conf. Ser. **41**, 151 (2006).

[57] H. Fesefeldt. Preprint PITHA-85/02, RWTH Aachen, 1985.

[58] M. Bleicher *et al.*, J. Phys. G: Nucl. Part. Phys. **25**, 1859 (1999).

[59] A. Mücke, R. Engel, J. P. Rachen, R. J. Protheroe, and T. Stanev, Comput. Phys. Commun. **124**, 290 (2000), `astro-ph/9903478`.

[60] H.-J. Drescher, M. Bleicher, S. Soff, and H. Stoecker, Astropart. Phys. **21**, 87 (2004), `astro-ph/0307453`.

[61] C. Meurer, J. Bluemer, R. Engel, A. Haungs, and M. Roth, Czech. J. Phys. **56**, A211 (2006), `arXiv:astro-ph/0512536`.

[62] P. D. B. Collins, *An Introduction to Regge Theorie & High Energy Physics,*. Cambridge University Press,, Cambridge, 1977.

[63] V. N. Gribov, Sov. Phys. JETP **26**, 414 (1968).

[64] N. N. Kalmykov and S. S. Ostapchenko, Phys. Atom. Nucl. **56**, 346 (1993).

[65] N. N. Kalmykov, S. S. Ostapchenko, and A. I. Pavlov, Nucl. Phys. Proc. Suppl. **52B**, 17 (1997).

[66] S. Ostapchenko, Phys. Rev. **D74**, 014026 (2006), `arXiv:hep-ph/0505259`.

[67] S. Ostapchenko, Phys. Lett. **B636**, 40 (2006), `arXiv:hep-ph/0602139`.

[68] R. S. Fletcher, T. K. Gaisser, P. Lipari, and T. Stanev, Phys. Rev. **D50**, 5710 (1994).

[69] R. Engel, T. K. Gaisser, T. Stanev, and P. Lipari. Prepared for 26th International Cosmic Ray Conference (ICRC 99), Salt Lake City, Utah, 17-25 Aug 1999.

[70] K. Werner, F.-M. Liu, and T. Pierog, Phys. Rev. **C74**, 044902 (2006), `arXiv:hep-ph/0506232`.

[71] T. Pierog and K. Werner, Phys. Rev. Lett. **101**, 171101 (2008), `arXiv:astro-ph/0611311`.

[72] J. Ranft, Phys. Rev. **D51**, 64 (1995).

[73] S. Roesler, R. Engel, and J. Ranft, *The Monte Carlo event generator DPMJET-III at cosmic ray energies* (unpublished). Prepared for 27th International Cosmic Ray Conference (ICRC 2001), Hamburg, Germany, 7-15 Aug 2001, p. 439.

[74] F. W. Bopp, J. Ranft, R. Engel, and S. Roesler, Phys. Rev. **C77**, 014904 (2008), `hep-ph/0505035`.

[75] M. Zha, J. Knapp, and S. Ostapchenko (2003). Prepared for 28th International Cosmic Ray Conference (ICRC 2003), Tsukuba, Japan, 31 Jul - 7 Aug 2003, p. 515-518.

[76] R. Engel, Nucl. Phys. Proc. Suppl. **122**, 40 (2003).

[77] V. Topor Pop, M. Gyulassy, and H. Rebel, Astropart. Phys. **10**, 211 (1999), `nucl-th/9809014`.

[78] M. Gyulassy and X.-N. Wang, Comput. Phys. Commun. **83**, 307 (1994), `arXiv:nucl-th/9502021`.

[79] R. Luna, A. Zepeda, C. A. Garcia Canal, and S. J. Sciutto, Phys. Rev. **D70**, 114034 (2004), `hep-ph/0408303`.

[80] H.-J. Drescher and G. R. Farrar, Astropart. Phys. **19**, 235 (2003), `hep-ph/0206112`.

[81] T. K. Gaisser, R. J. Protheroe, K. E. Turver, and T. J. L. Mccomb, Rev. Mod. Phys. **50**, 859 (1978).

[82] KASCADE Collaboration, T. Antoni *et al.*, Nucl. Instrum. Meth. **A513**, 490 (2003).

[83] Pierre Auger Collaboration, J. Abraham *et al.*, Nucl. Instrum. Meth. **A523**, 50 (2004).

[84] KASCADE Collaboration, T. Antoni *et al.*, Astropart. Phys. **16**, 245 (2002), `astro-ph/0102443`.

[85] J. R. Hörandel, J. Phys. **G29**, 2439 (2003), `astro-ph/0309010`.

[86] HiRes Collaboration, T. Abu-Zayyad *et al.*, Nucl. Instrum. Meth. **A450**, 253 (2000).

[87] Pierre Auger Collaboration, R. Engel (2007), `arXiv:0706.1921 [astro-ph]`.

[88] Pierre Auger Collaboration, A. S. Chou *et al.* Proc. of 29th Int. Cosmic Ray Conference (ICRC 2005), Pune, India, 3-11 Aug 2005, p. 319.

[89] F. Schmidt, M. Ave, L. Cazon, and A. S. Chou, Astropart. Phys. **29**, 355 (2008), `arXiv:0712.3750 [astro-ph]`.

[90] H. J. Drescher, A. Dumitru, and M. Strikman, Phys. Rev. Lett. **94**, 231801 (2005), `arXiv:hep-ph/0408073`.

[91] R. Engel, Nucl. Phys. B (Proc. Suppl.) **75A**, 62 (1999), `astro-ph/9811225`.

[92] M. Albrow *et al.*, *Prospects for diffractive and forward physics at the LHC* (unpublished). CERN-LHCC-2006-039, CMS Note-2007/002, TOTEM Note 06-5.

[93] T. Sako *et al.*, Nucl. Instrum. Meth. **A578**, 146 (2007).

[94] UA7 Collaboration, E. Pare *et al.*, Phys. Lett. **B242**, 531 (1990).

[95] CDF Collaboration, F. Abe *et al.*, Phys. Rev. **D50**, 5550 (1994).

[96] E710 Collaboration, N. A. Amos *et al.*, Phys. Rev. Lett. **63**, 2784 (1989).

[97] E811 Collaboration, C. Avila *et al.*, Phys. Lett. **B445**, 419 (1999).

[98] SELEX Collaboration, U. Dersch *et al.*, Nucl. Phys. **B579**, 277 (2000), `arXiv:hep-ex/9910052`.

[99] R. J. Glauber and G. Matthiae, Nucl. Phys. **B21**, 135 (1970).

[100] R. Ulrich, J. Blümer, R. Engel, F. Schüssler, and M. Unger (2007), `arXiv:0709.1392 [astro-ph]`. In Proc. of 12th Int. Conf. on Elastic and Diffractive Scattering, Hamburg, May 21 - 25, 2007.

[101] C. Pajares, D. Sousa, and R. A. Vazquez, Phys. Rev. Lett. **86**, 1674 (2001), `arXiv:astro-ph/0005588`.

[102] J. Dias de Deus, M. C. Espirito Santo, M. Pimenta, and C. Pajares, Phys. Rev. Lett. **96**, 162001 (2006), `arXiv:hep-ph/0507227`.

[103] J. Alvarez-Muniz *et al.*, Astropart. Phys. **27**, 271 (2007), `hep-ph/0608050`.